Characterisation of the deflection of a liquid jet in an annular flow

M. Birouk, M. Menacer, G. Ishaq, A. Aroussi, B.J. Azzopardi

Rolls-Royce Nottingham University Technology Centre

School of Mechanical, Materials, Manufacturing Engineering and Management

University of Nottingham, NG7 2RD, England

ABSTRACT

An experimental study of a water jet deflection in an annular flow, driven by a rotating cylinder, in a stationary casing is presented. The apparatus consists of a rotating cylinder (600 mm long and 60 mm in diameter) connected to a motor capable of generating speeds ranging from 0 to 3000 rpm. A stationary casing of 127 mm diameter, made of clear Perspex, surrounds the cylinder. The liquid (in this study water) is injected through the apparatus via a flexible pipe connected to a tank located at the top of the rig and is supplied as a continuous laminar jet into the casing so that it impinges on the cylinder and breaks-up into droplets with different sizes. These are then deflected by the effect of the rotating cylinder as discontinuous jets of droplets with different size towards the stationary casing. The injected water flow rates are varied up to 0.38 l/min and the cylinder speeds up to 3000 rpm.

Particle Imaging Velocimeter PIV) is used to scrutinise the flow events. The equipment used to generate the pulsed light sheets consists of a twin pulsed Nd:YAG lasers, operating at 15 Hz. The laser system is Q-switched to provide 150 mJ of pulse maximum energy at 532 nm, and the pulse duration is 4 ns. The advantage of this system is that the pulse separation can be altered to the desired value for the particular flow properties under examination. This feature is crucial for the capture of the real structure of the flow phenomena under investigation. To image the flow field in the area of interest, a Megaplus Kodak camera model ES1.0 of 1008 x 1018 pixel resolution with a 50 mm Nikon imaging lens was placed perpendicular to the laser sheet. The laser and the camera were synchronised via a DANTEC PIV 2100 processor. A Personal Computer is used to collect, store and process the data.

This investigation is primarily concerned with the effect of a rotating annular flow on a freely falling water jet, which impinges on a rotating cylinder and then deflects within the gap between the cylinder and the stationary casing. The annular flow velocity profile of the gas phase (air) was obtained using PIV and LDV; it reveals that the airflow tangential velocity decreases along the distance across the gap from the cylinder to the casing and increases as the cylinder rotation speed increases.

The major findings of this study are:

- Increasing the jet flow rate causes an increase in droplet generation at the point of impingement. Moreover, higher flow rates affect the flow structure as a result of the enhanced water film breaking-up into droplets of different sizes, which are then deflected by the rotating surface of the cylinder.

- Increasing the cylinder speed appears to enhance the break-up of the water film around the rotating cylinder (due to increased Weber number). The breaking film forms droplets that are then deflected by the rotating surface of the cylinder/shaft.

- It is observed that the surrounding air entrains new droplets from the jet itself, as well as from the water film deposited on the internal surface of the stationary casing.

- The deflection of the liquid jet from vertical, at the rotating shaft surface, increases with increasing the cylinder rotational speed and decreases with increasing the liquid flow rate.

- The scattering/expansion angle of the deflection of the “secondary” jets is larger/wider at lower cylinder rotational speed.

1. INTRODUCTION

The presence of air and oil in gas turbines bearing chambers with walls rotating at high speed can result in oil fires as well as the deterioration of the lubrication function of the oil. Oil within the bearing chamber can exist as a distribution of droplets ranging in size from a few up to many hundreds of microns, within the core flow, and as a film of varying thickness on the enclosing walls. The dynamics of oil droplets within a gas flow are governed by a number of factors, each of whose importance is dependent on drop size, drop density and gas flow conditions. Another important differentiating factor in the case of a bearing chamber are the centrifugal accelerations generated by the rapidly rotating boundaries. As temperatures and pressures inside modern engines increase so the problem of heat management increases. In order to optimise the design and performance of engine heat management systems it is essential to identify and understand the sources of heat generation and removal.

The lubricating oil is injected through a nozzle jet into the bearing chamber where it impinges onto a rotating shaft and is subsequently deflected, or broken-up. A fraction of the pressurized air, which is provided to seal the bearing chamber, enters into the chamber and mixes with the lubrication oil flow. At the exit of the jet, a spray of oil-droplets of different sizes impinges onto a rotating oil film, which is created on the rotating shaft. In this case and depending on the flow dynamic conditions, many scenarios may happen; the liquid drops impinging on the rotating film may be absorbed into the film or may splash to form new droplets which may further break-up into smaller droplets while rotating around the shaft or coalesce together to form larger oil droplets. It is also possible that at very high rotating speed, the surrounding air may shear-off and entrain new oil droplets from the rotating oil film as well as from the liquid jet itself.

Numerous experimental studies have been carried out to gain insight into the above-mentioned scenarios by isolating each parameter and using simple experimental sets-up. Several publications can be found in the literature. For example the impact of drops on walls/surfaces and films was reported by Tropea and Marengo (1999), and Samenfink et al (1999). The phenomenon of droplet collision was investigated by Sikdar and Chung (1997), whilst the mechanism of droplet splashing was reported by Martin and Frohn (1999). The transitional regime between coalescing and splashing drops was studied by Rein (1996).

In the present experimental study, the rotating component is modelled as a cylindrical shaft and the lubricating jet is simplified as a water jet, which is injected from the surrounding static casing on to the shaft. The main aim of the study is to gain an insight into the interaction of liquid and air and the flow regimes induced by the rotating cylinder. A parametric study is conducted by varying independently the liquid-jet flow rate and the cylinder rotational speed. The PIV technique has been selected as the flow diagnostic tool. This technique, as the name implies, uses particles as the seeding material, within the main flow of interest. The particles in the field of interest are illuminated by two sheets of laser light that are separated by a specified time delay, and the scattered light off the particles is collected on a photographic image plane oriented 90 degrees to the laser sheet. The theory, application and limitations of the PIV technique are well documented in the literature (Raffel et al., 1997 and Grant, 1997).

2. METHODOLOGY

2.1. Apparatus

A schematic layout of the experimental set-up used in this investigation is shown in Figure 1. The apparatus consists of a rotating cylinder (600 mm long and 60 mm in diameter) capable of rotational speeds ranging from 0 to 3000 rpm. The rotating cylinder is surrounded by a stationary casing of 127 mm of diameter, made of clear Perspex. The liquid, in this case water, is supplied into the apparatus via a flexible pipe connected to a tank located at the top of the rig and is injected as a continuous laminar jet into the casing to impinge onto the rotating cylinder (Fig 1). The water flow rates chosen for this investigation from 0 to 0.38 l/min and the shaft speeds are from stationary to 3000 rpm.

2.2. Optical set-up

The PIV technique is used since it provides good accuracy, resolution and reliability for the instantaneous qualitative and quantitative measurements of a whole flow field. The anemometer generates the light sheets from a twin pulsed Nd:YAG lasers, operating at 15 Hz. The laser system is Q-switched to provide 150 mJ of pulse maximum energy at 532 nm, and the pulse duration is 4 ns. The advantage of this tandem system is that the pulse

separation can be altered to any desired value. This pulse separation control is crucial as it is responsible for capturing the real structure of the flow. For instance, if this time is greater than the Taylor or dissipation scales of the flow, the PIV would only provide information of the flow at macro-scale level. To capture the flow images, the optical recording device used is a Kodak ES 1.0 CCD camera with a 60mm lens. The camera resolution is 1008x1018 array pixels, with 256 grey levels. The laser and the camera are synchronised via a DANTEC PIV 2100 processor. A PC is used to collect, store and process data.

The single-phase airflow within the rig enclosure has also been measured with a two component Laser Doppler Velocimeter (LDV). This is in order to correlate between the time averaged LDV data and the PIV data which is averaged through the interrogation of a series of images taken for a given set of experimental conditions. The LDV system consists of a 1W Argon Ion laser, integrated transmitter/receiver probe; Bragg cells for frequency bias and Burst Spectrum Analysers for signal analysis and flow properties extraction.

2.3. Test procedure

First, the water flow rate is selected then the motor is turned on to drive the cylinder up to the selected rotational speed. After the annular flow has reached its steady state conditions, the acquisition system is then activated to allow imaging of the flow. The experiments are repeated several times for the same experimental conditions in order to achieve statistical consistency of the results. Some preliminary PIV tests are usually done to calibrate the experimental set-up and to ensure that the pulse separation is set to the optimum value and that the water droplets are discernible in the images. These tests repeated when the experimental conditions, such as the cylinder rotational speed and water flow rate, change.

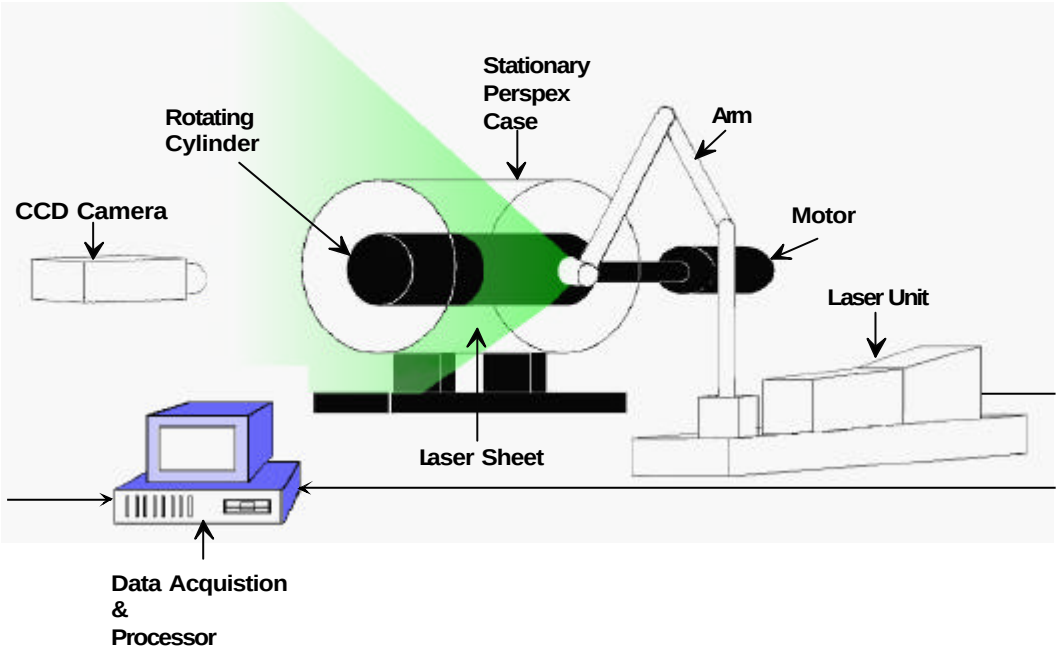

Figure 1: The experimental set-up and associated instrumentation

3. RESULTS AND DISCUSSION

A photographic image of the flow in the gap where the water jet is injected from the top, down onto the rotating cylinder, is shown in figure 2. This is a typical image of the water jet as deflected by the rotating cylinder but the image does not show the flow behaviour behind the cylinder, that is the darker side, due to the light blockage effect. When the laser light is provided all around the cylinder the flow pattern generated by water shedding and entrainment is depicted in figure 3. All the PIV flow-field images are obtained with a fixed field of view of 75 mm (horizontal) by 75 mm (vertical), which is the size of the right quadrant of the test section sketched in figure 3, having the jet on the left hand side of the field of view. Figure 3 shows the area of the test rig section particularly scrutinised. A definition of the scattering angle of the secondary jets is also shown in this figure.

Although the whole test rig section has been imaged using PIV and visualisation techniques, the present paper presents only results dealing with the jet characterisation within the first quadrant, shown in Figure 3. More results on the behaviour of the flow all around the cylinder in the gap are provided in subsequent publications.

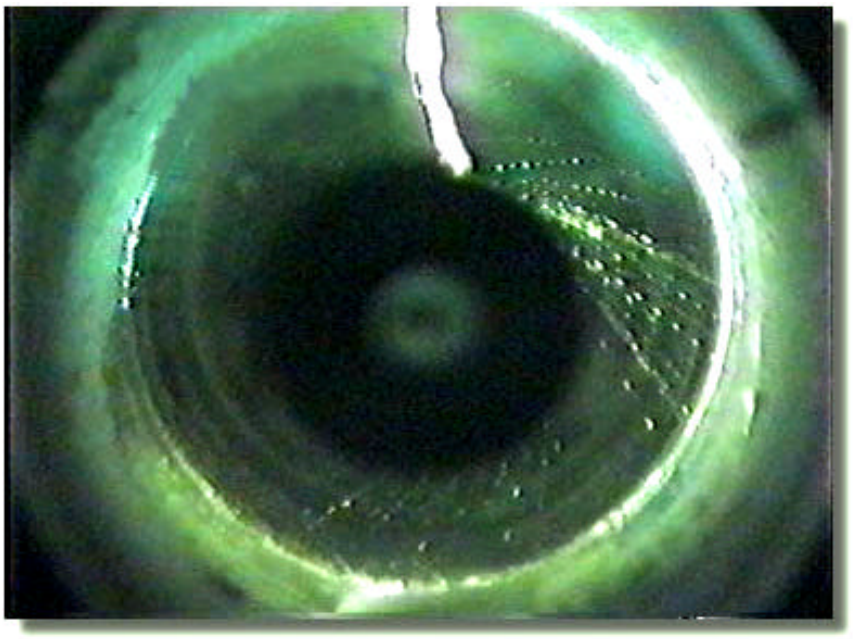

Figure 2: Typical flow visualisation image of the jet deflection.

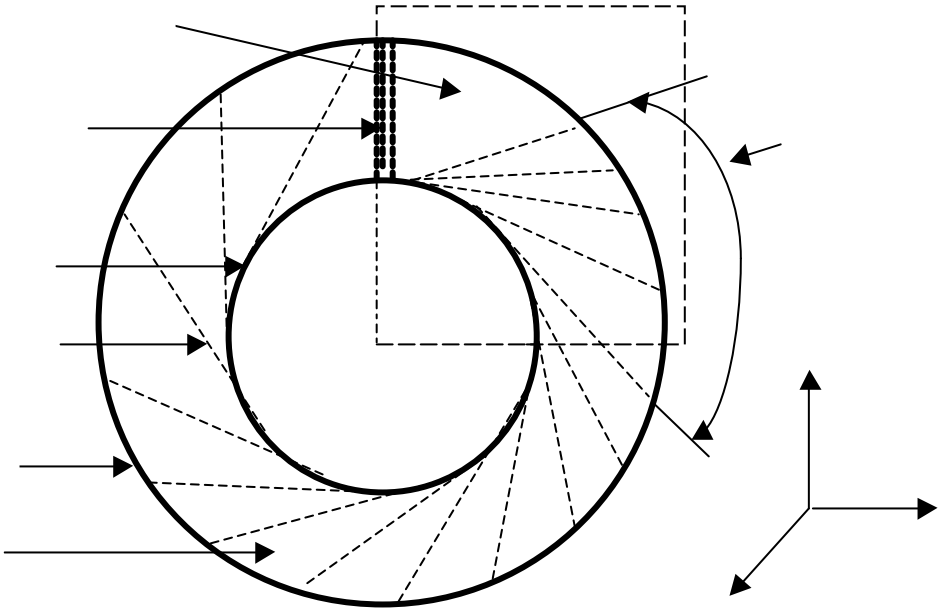

Figure 3: Sketch of the rig test section.

3.1. Gas-phase velocity profile

The gas-phase (that is air) velocity profile of the annular flow is obtained by analysing the PIV cross-correlation images. LDV data is also acquired for validation purposes. The variation of the tangential velocity within the gap between the cylinder and the casing is shown in Figure 4. This figure shows that the tangential velocity of the air-phase, at the two shaft speeds displayed, decreases with increased distance away from the rotating surface. This is self-explanatory since the rotating cylinder entrains more air in the vicinity of its moving boundary. This effect then subsides with increased radial distance until the flow comes to a halt at the stationary surface. It shows also that increasing the rotational speed of the cylinder yields a significant increase of the air velocity for the same distance in the gap.

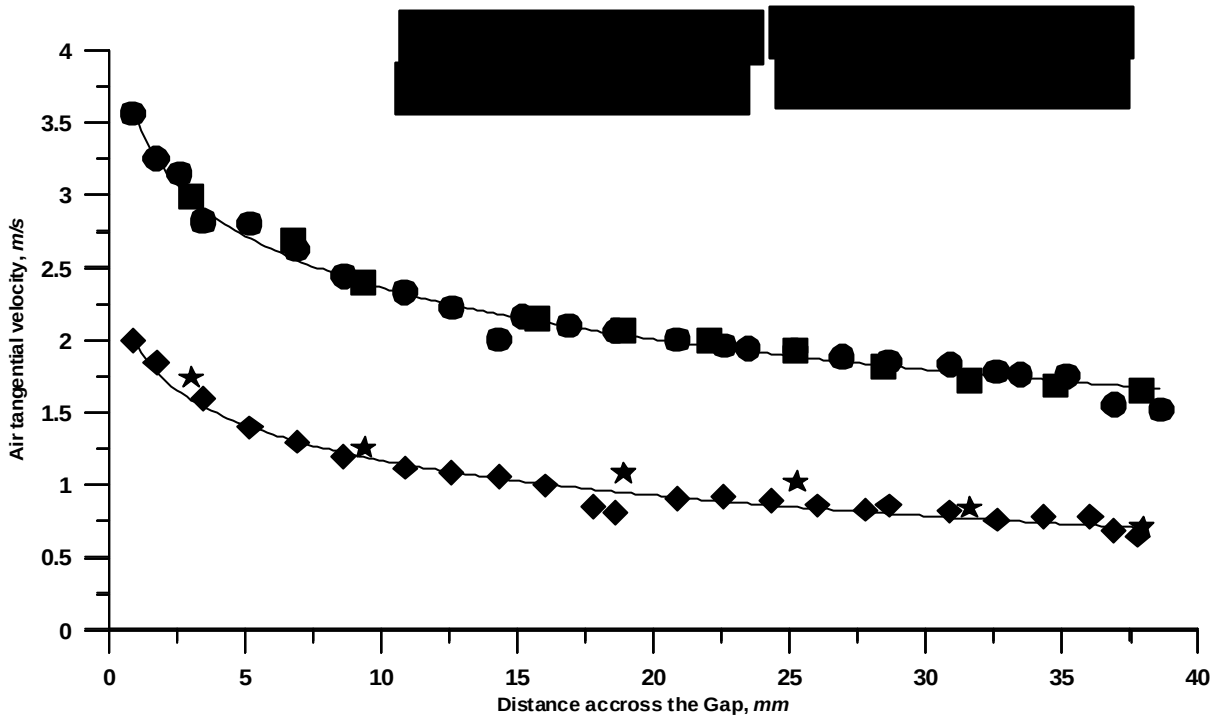

Figure 4: Gas phase tangential velocity profile.

3.2. Averaged velocity vectors

In order to identify the effects of the jet discharge speed on the flow around the rotating cylinder, two PIV images of the flow in the gap between the rotating cylinder and the stationary casing are presented in figure 5. The latter, shows that by increasing the discharge flow rate (or speed) of the jet, the spatial distribution of droplets across the gap is increased. This can be explained by the fact that the jet at higher flow rate carries more water mass to impinge on the surface of the rotating cylinder and hence more water droplets are born by the deflection and windage effects. The rotating cylinder surface and the tangential velocity of the flow are responsible for the break-up of the liquid film into droplets with different sizes as shown in figure 5. To support this explanation a comparison is made between the two figures of the averaged velocity vectors presented in figure 6, where at higher jet flow rate the overall movement of the flow is affected as a result of the increased density of droplets, which are then deflected.

The second parameter, which is also investigated here, concerns the cylinder rotational speed. Figure 7 shows a PIV image and its corresponding averaged velocity vector map at the conditions stated in the figure. This figure also shows that for a given jet discharge flow rate, the increase in the cylinder speed affects the droplets spatial distribution/density in the gap between the rotating cylinder and the stationary casing. This supports the theory that increasing the shaft speed, namely increasing the Weber number, enhances the droplets break-up (compare

figure 5a with figure 7a). By comparing the vector fields of figure 6a with figure 7b, it is easy to see the cause of the enhanced jet deflection.

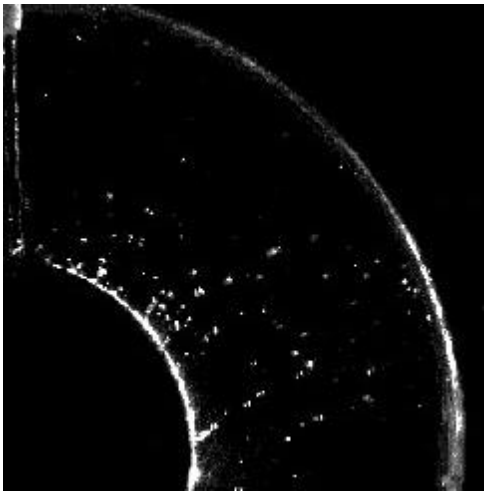

Fig. 5a (N=1300 rpm, Q=0.22 l/min)

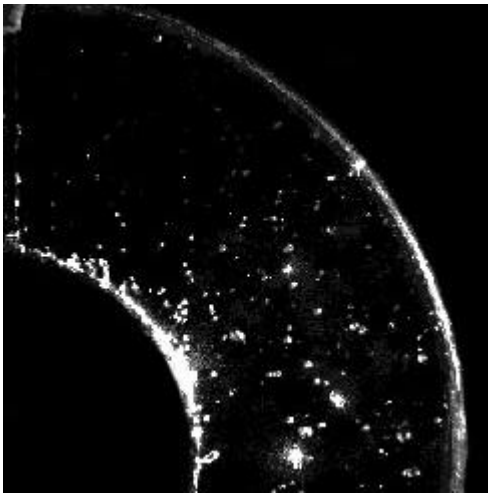

Fig. 5b (N=1300 rpm, Q=0.38 l/min)

Figure 5: PIV images of the flow-filed in the area of interest.

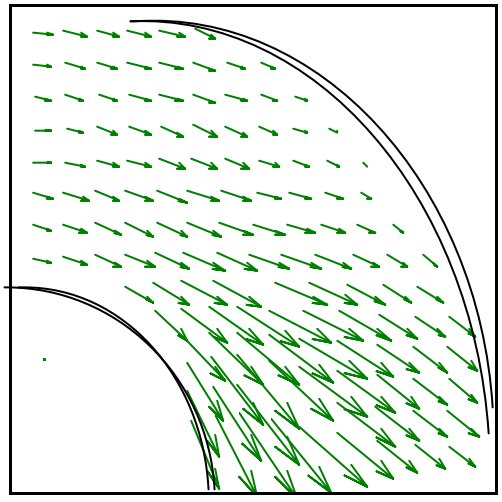

Fig. 6a (N=1300 rpm, Q=0.22 l/min)

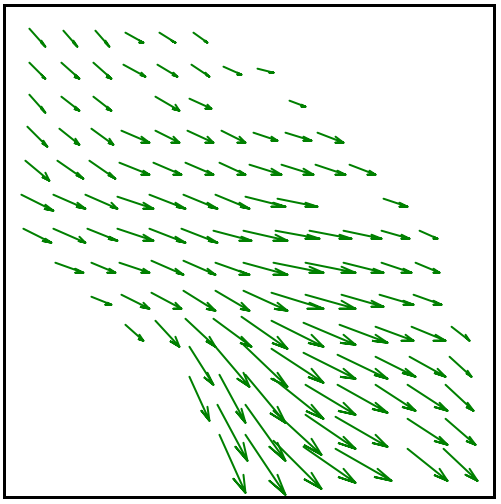

Fig. 6b (N=1300 rpm, Q=0.38 l/min)

Figure 6: Averaged velocity field obtained by PIV

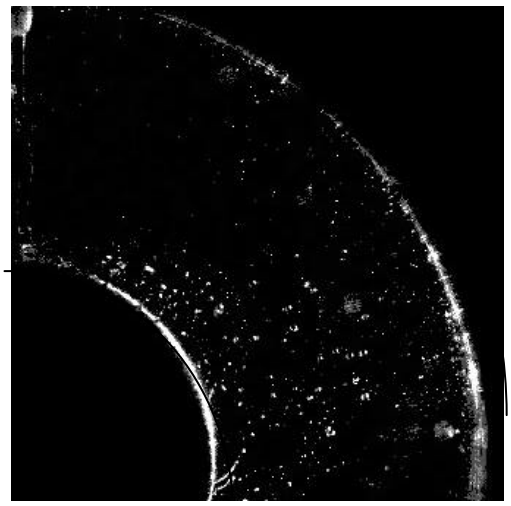

Fig. 7a (N=3000 rpm, Q=0.22 l/min)

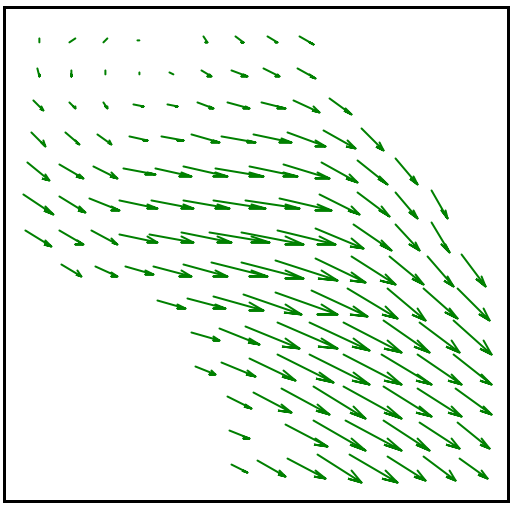

Fig. 7b (N=3000 rpm, Q=0.22 l/min)

Figure 7: PIV image (7a), and averaged velocity field (7b).

3.3. Jet deflection

The deviation of the jet from its vertical position has been measured from the visualisation images and averaged at different cylinder rotation speeds and water flow rates explored in this investigation. Figure 8 shows how the water jet deflection varies with cylinder speed at two different water flow rates of 0.22 l/min and 0.38 l/min respectively. The casing is sealed from both sides and thus no external swirl of the air is possible. The air circulation with the rotating cylinder causes windage effect, which deflects the jet from its undisturbed position. As the cylinder speed increases, the windage speed increases and thus the jet deviation/deflection also increases. However, this increase is less important in the case of higher flow rates. This is because higher flow rates give higher resistance to the windage forces and thus yield lower jet deflection/deviation. Furthermore, at higher liquid jet flow rates and higher shaft rotational speeds, the jet acts as a cylinder in a cross flow and results in vortex shedding on its downstream side as can be seen from figures 6b and 7b. This phenomenon is observed visually during the experiment where the jet oscillates in the cross flow due to the aforementioned vortex shedding.

It is important to notice here that in addition to the cylinder rotation speed and water flow rates which affect drastically the deflection of the principle water jet there it is also possible that the shape of the cylinder surface (roughness) would be a non negligible parameter to consider. However, no attempts have been made to look at the effect of this parameter in this paper.

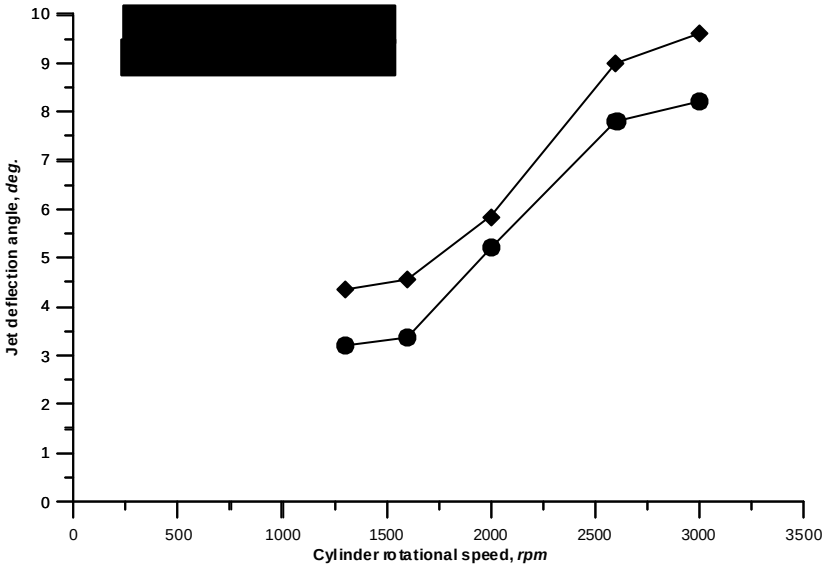

Figure 8: Jet deflection of the principal jet versus the cylinder rotation speed

3.4. Scattering/expansion angle of "secondary" jets

A qualitative analysis, has also been conducted, of the visualisation images of the "principal" water jet impinging on the rotating cylinder which then breaks into different jets. These jets are then deflected at different angles as shown in the figure 9. The full angle is called the scattering/expansion angle as it is defined in figure 3.

Two typical images are presented in Figure 9. The two images are obtained at the same water jet flow rate and two different rotational cylinder speeds. These two images show clearly the effect of increasing the cylinder rotational speed on the scattering / expansion angle of the jets.

As an example of this scattering effect, a typical variation of the scattering angle, for a constant flow rate of 0.22 l/min, are plotted against the cylinder speed as shown in figure 10. At quenching conditions the water flows around the cylinder without any deflection. However, as the cylinder rotational speed increases the scattering/expansion angle increases until it reaches a maximum of approximately 40 degrees at rotational speed of 1300 rpm, then it decreases to a value of just around 20° at 3000 rpm, this is shown in figure 10. The reason for the decrease in the scattering angle at higher rotational speeds could be due to the increase of the windage tangential velocity. This is clearly illustrated in figure 4 where the air tangential velocity increases as the rotational speed increases. This exercises a higher tangential stream force on the deflected secondary jets and forces these jets to change their direction downwards. In other word, the drag coefficient of these droplets diminishes as the annular flow velocity increases so that the flow is able to carry these droplets or deflect them downstream of the flow.

Figure 10 shows some scatter in the data; this is more probably caused in part by the vibrations of the shaft at higher rotational speed, but more important due to the jet oscillation caused by the vortex shedding effect described earlier.

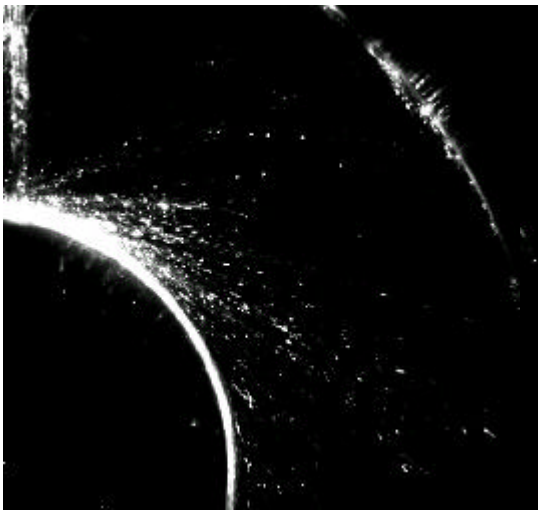

(N=1300 rpm, Q=0.38 l/min)

Figure 9: Scattering angle changes with the rotational speed

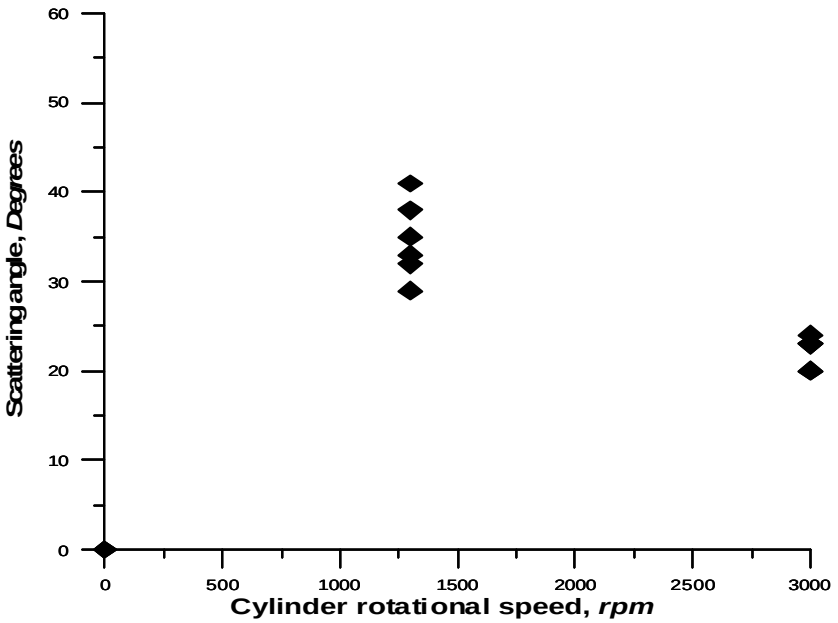

Figure 10: Scattering/expansion angle of the "secondary" jets versus the cylinder rotational speed

4. SUMMARY AND CONCLUSIONS

The impingement and break-up of a liquid jet on a rotating cylinder/shaft in an annular flow has been investigated. The injected water onto the rotating cylinder is then deflected as an ensemble of discontinuous jets with different angles; these jets are composed of different droplets sizes. Some of these "secondary" jets of droplets hit the wall of the stationary casing and break-up into even smaller droplets.

The present investigation used Particle Image Velocimetry (PIV) and Laser Doppler Velocimetry (LDV) to scrutinise the flow events within the annular enclosure. These non-intrusive techniques are able to map the flow field and provide complimentary both instantaneous as well as average information.

The general major concluding remarks of this work on jet deflection behaviour are:

- Increasing the jet flow rate causes an increase in droplet generation at the point of impingement. Moreover, higher flow rates affect the flow structure as a result of the enhanced water film breaking-up into droplets of different sizes, which are then deflected by the rotating surface of the cylinder.

- Increasing the cylinder speed appears to enhance the break-up of the water film around the rotating cylinder (due to increased Weber number). The breaking film forms droplets that are then deflected by the rotating surface of the cylinder/shaft.

- It is observed that the surrounding air entrains new droplets from the jet itself, as well as from the water film deposited on the internal surface of the stationary casing.

- The deflection of the liquid jet from vertical, at the rotating shaft surface, increases with increasing the cylinder rotational speed and decreases with increasing the liquid flow rate.

- The scattering/expansion angle of the deflection of the "secondary" jets is larger/wider at lower cylinder rotational speed.

ACKNOWLEDGEMENTS

The authors would like to acknowledge the financial support from Rolls Royce plc through the funding of the UTC at Nottingham.

REFERENCES

Glahn A., Kurreck M., Willman M., Witting S. (1995). "Feasibility study on oil droplet flow investigations inside aero engine bearing chambers: PDA technique in combination with numerical approaches", ASME Paper No.95-GT-100.

Grant, I. (1997). "Particle Image Velocimetry: a review". Proc. Instn. Mech. Engrs. 211, pp. 55-76.

Martin R., Frohn A. (1999). "A numerical study on the mechanism of splashing". Int. J. of Heat and Fluid Flow 20, 455-461.

Raffel M., Willert C., Kompenhans J. (1997). "Particle Image Velocimetry". Springer-verlag.

Rein, M. (1996). "The transitional regime between coalescing and splashing drops". J. Fluid Mech., 306, pp. 145-165.

Samenfink W., Elsaber A., Dullenkopf K., Wittig S. (1999). "Droplet interaction with shear-driven liquid films: anlysis of deposition and secondary droplet characteristics". Int. J. of Heat and Fluid Flow, 20, pp. 462-469

Sikdar S., Chung J.N. (1997). "A Quasimolecular approach for discrete study of droplet collision". IJCFD, 8, pp. 189-200.

Tropea C., Marengo M. (1999). "The impact of drops on walls and films". Multiphase Science and Technology, 11, pp. 19-36.

Wittig S., Glahn A., Himmelsbach (1993). "Influence of high rotational speeds on heat and oil film thickness in aero-engine bearing chambers". ASME Paper No. 93-GT-209.

Wittig S. (1990). "Heat transfer analysis in rotating gas turbine components: experimental and non-intrusive diagnostics". 3rd International Symposium on Transport Phenomena and Dynamics of Rotating Machinery. USA.